

An efficient algorithm for 1-dimensional (persistent) path homology

Tamal K. Dey ^{*1}, Tianqi Li ^{†1}, and Yusu Wang^{‡1}

¹ Department of Computer Science and Engineering, The Ohio State University, Columbus

January 29, 2020

Abstract

This paper focuses on developing an efficient algorithm for analyzing a directed network (graph) from a topological viewpoint. A prevalent technique for such topological analysis involves computation of homology groups and their persistence. These concepts are well suited for spaces that are not directed. As a result, one needs a concept of homology that accommodates orientations in input space. Path-homology developed for directed graphs by [11] has been effectively adapted for this purpose recently by Chowdhury and Mémoli [6]. They also give an algorithm to compute this path-homology. Our main contribution in this paper is an algorithm that computes this path-homology and its persistence more efficiently for the 1-dimensional (H_1) case. In developing such an algorithm, we discover various structures and their efficient computations that aid computing the 1-dimensional path-homology. We implement our algorithm and present some preliminary experimental results.

1 Introduction

When it comes to graphs, traditional topological data analysis has focused mostly on undirected ones. However, applications in social networks [2, 20], brain networks [25], and others require processing directed graphs. Consequently, topological data analysis for these applications needs to be adapted accordingly to account for directedness. Recently, some work [5, 19] have initiated to address this important but so far neglected issue.

Since topological data analysis uses persistent homology as a main tool, one needs a notion of homology for directed graphs. Of course, one can forget the directedness and consider the underlying undirected graph as a simplicial 1-complex and use a standard persistent homology pipeline for the analysis. However, this is less than desirable because the important information involving directions is lost. Currently, there are two main approaches that have been proposed for dealing with directed graphs. One uses directed clique complexes [9, 19] and the other uses the concept of path homology [11]. In the first approach, a k -clique in the input directed graph is turned into a $(k - 1)$ -simplex if the clique has a single source and a single sink. The resulting simplicial complex is subsequently analyzed with the usual persistent homology pipeline. One issue with this approach is that there could be very few cliques with the required condition and thus accommodating only a very few higher dimensional simplices. In the worst case, only the undirected graph can be returned as the directed clique complex if each 3-clique is a directed cycle.

*tamaldehy@cse.ohio-state.edu

†li.6108@osu.edu

‡yusu@cse.ohio-state.edu

The second approach based on path homology alleviates this deficiency. Furthermore, certain natural functorial properties, such as Künneth formula, do not hold for the clique complex [11].

The path homology, originally proposed by Grigoryan, Lin, Muranov and Yau in 2012 [11] and later studied by [6, 12, 13], has several properties that make it a richer mathematical structure. For example, there is a concept of homotopy under which the path homology is preserved; it accommodates Künneth formula; and the path homology theory is dual to the cohomology theory of digraphs introduced in [13]. Furthermore, persistent path homology developed in [6] is shown to respect a stability property for its persistent diagrams.

To use path homologies effectively in practice, one needs efficient algorithms to compute them. In particular, we are interested in developing efficient algorithms for computing 1-dimensional path homology and its persistent version because even for this case the current state of the art is far from satisfactory: Given a directed graph G with n vertices, the most efficient algorithm proposed in [6] has a time complexity $O(n^9)$ (more precisely, their algorithm takes $O(n^{3+3d})$ to compute the $(d-1)$ -dimensional persistent path-homology).

The main contribution of this paper is stated in Theorem 1.1. The reduced time complexity of our algorithm can be attributed to the fact that we compute the boundary groups more efficiently. In particular, it turns out that for 1-dimensional path homology, the boundary group is determined by bigons, certain triangles, and certain quadrangles in the input directed graph. The bigons and triangles can be determined relatively easily. It is the boundary quadrangles whose computation and size determine the time complexity. The authors in [6] compute a basis of these boundary quadrangles by constructing a certain generating set for the 2-dimensional chain group by a nice column reduction algorithm (being different from the standard simplicial homology, it is non-trivial to do reduction for path homology). We take advantage of the concept of *arboricity* and related results in graph theory, together with other efficient strategies, to enumerate a much smaller set generating the boundary quadrangles. Computing the cycle and boundary groups efficiently both for non-persistent and persistent homology groups is the key to our improved time complexity.

Theorem 1.1. *Given a directed graph G with n vertices and m edges, set $r = \min\{\mathbf{a}(G)m, \sum_{(u,v) \in E} (d_{in}(u) + d_{out}(v))\}$, where $\mathbf{a}(G) = O(n)$ is the so-called arboricity of G , and $d_{in}(u)$ and $d_{out}(u)$ are the in-degree and out-degree of u , respectively. There is an $O(rm^{\omega-1} + m\alpha(n))$ time algorithm for computing the 1-dimensional persistent path homology for G where $\omega < 2.373$ is the exponent for matrix multiplication¹, and $\alpha(\cdot)$ is the inverse Ackermann function.*

This also gives an $O(rm^{\omega-1} + m\alpha(n))$ time algorithm for computing the 1-dimensional path homology H_1 of G .

In particular, for a planar graph G , $\mathbf{a}(G) = O(1)$ and the time complexity becomes $O(n^\omega)$.

The *arboricity* $\mathbf{a}(G)$ of a graph G mentioned in Theorem 1.1 denotes the minimum number of edge-disjoint spanning forests into which G can be decomposed [14]. It is known that in general, $\mathbf{a}(G) = O(n)$, but it can be much smaller. For example, $\mathbf{a}(G) = O(1)$ for planar graphs and $\mathbf{a}(G) = O(g)$ for a graph embedded on a genus- g surface [4]. Hence, for planar graphs, we can compute 1-dimensional persistent path homology in $O(n^\omega)$ time whereas the algorithm in [6] takes $O(n^5)$ time².

Organization of the paper. After characterizing the 1-dimensional path homology group H_1 in Section 3, we first propose a simple algorithm to compute it. In Section 4, we consider its persistent version and present an improved and more efficient algorithm. In Section 5, we

¹That is, the fastest algorithm to multiply two $r \times r$ matrices takes time $O(r^\omega)$.

²The original time complexity stated in the paper is $O(n^9)$ for 1-dimensional case. However, one can improve it to $O(n^5)$ by a more refined analysis for planar graphs.

develop an algorithm to compute 1-dimensional *minimal path homology basis* [8, 10], and also show experiments demonstrating the efficiency of our new algorithms.

2 Background

We briefly introduce some necessary background for path homology. Interested readers can refer to [11] for more details. The original definition can be applied to structures beyond directed graphs; but for simplicity, we use directed graphs to introduce the notations.

Given a directed graph $G = (V, E)$, we denote (u, v) as the directed edge from u to v . A *self-loop* is defined to be the edge (u, u) from u to itself. Throughout this paper, we assume that G does not have self-loops. We also assume that G does not have multi-edges, i.e. for every ordered pair u, v , there is at most one directed edge from u to v . For notational simplicity, we sometimes use index i to refer to vertex $v_i \in V = \{v_1, \dots, v_n\}$.

Let \mathbb{F} be a field with 0 and 1 being the additive and multiplicative identities respectively. We use $-a$ to denote the additive inverse of a in \mathbb{F} . An *elementary d -path* on V is simply a sequence i_0, i_1, \dots, i_d of $d+1$ vertices in V . We denote this path by e_{i_0, i_1, \dots, i_d} . Let $\Lambda_d = \Lambda_d(G, \mathbb{F})$ denote the \mathbb{F} -linear space of all linear combinations of elementary d -paths with coefficients from \mathbb{F} . It is easy to check that the set $\{e_{i_0, \dots, i_d} \mid i_0, \dots, i_d \in V\}$ is a basis for Λ_d . Each element p of Λ_d is called a *d -path*, and it can be written as

$$p = \sum_{i_0, \dots, i_d \in V} a_{i_0 \dots i_d} e_{i_0 \dots i_d}, \text{ where } a_{i_0 \dots i_d} \in \mathbb{F}.$$

Similar to simplicial complexes, there is a well-defined *boundary operator* $\partial : \Lambda_d \rightarrow \Lambda_{d-1}$:

$$\partial e_{i_0 \dots i_d} = \sum_{i_0, \dots, i_d \in V} (-1)^j e_{i_0 \dots \hat{i}_j \dots i_d},$$

where \hat{i}_k means the omission of index i_k . The boundary of a path $p = \sum_{i_0, \dots, i_d \in V} a_{i_0 \dots i_d} \cdot e_{i_0 \dots i_d}$, is thus $\partial p = \sum_{i_0, \dots, i_d \in V} a_{i_0 \dots i_d} \cdot \partial e_{i_0 \dots i_d}$. We set $\Lambda_{-1} = 0$ and note that Λ_0 is the set of \mathbb{F} -linear combinations of vertices in V .

Lemma 2.4 in [11] shows that $\partial^2 = 0$.

Next, we restrict to real paths in directed graphs. Specifically, given a directed graph $G = (V, E)$, call an elementary d -path e_{i_0, \dots, i_d} *allowed* if there is an edge from i_k to i_{k+1} for all k . Define \mathcal{A}_d as the space of all allowed d -paths, that is, $\mathcal{A}_d := \text{span}\{e_{i_0 \dots i_d} : e_{i_0 \dots i_d} \text{ is allowed}\}$. An elementary d -path $i_0 \dots i_d$ is called *regular* if $i_k \neq i_{k+1}$ for all k , and is *irregular* otherwise. Clearly, every allowed path is regular since there is no self-loop. However, the boundary map ∂ on Λ_d may create a term resulting into an irregular path. For example, $\partial e_{uvu} = e_{vu} - e_{uu} + e_{uv}$ is irregular because of the term e_{uu} . To deal with this case, the term containing consecutive repeated vertices is identified with 0 [11]. Thus, for the previous example, we get $\partial e_{uvu} = e_{vu} - 0 + e_{uv} = e_{vu} + e_{uv}$. The boundary map ∂ on \mathcal{A}_d is taken to be the boundary map for Λ_d restricted on \mathcal{A}_d with this modification: where all terms with consecutive repeated vertices created by the boundary map ∂ are replaced with 0's.

Unfortunately, after restricting to the space of allowed paths \mathcal{A}_* , the inclusion that $\partial \mathcal{A}_d \subset \mathcal{A}_{d-1}$ may not hold any more; that is, the boundary of an allowed d -path is not necessarily an allowed $(d-1)$ -path. To this end, we adopt a stronger notion of allowed paths: an allowed path p is *∂ -invariant* if ∂p is also allowed. Let $\Omega_d := \{p \in \mathcal{A}_d \mid \partial p \in \mathcal{A}_{d-1}\}$ be the space generated by all ∂ -invariant paths. We then have $\partial \Omega_d \subset \Omega_{d-1}$ (as $\partial^2 = 0$). This gives rise to the following *chain complex of ∂ -invariant allowed paths*:

$$\dots \Omega_d \xrightarrow{\partial} \Omega_{d-1} \xrightarrow{\partial} \dots \Omega_d \xrightarrow{\partial} \Omega_0 \xrightarrow{\partial} 0.$$

We can now define the homology groups of this chain complex. The d -th cycle group is defined as $Z_d = \text{Ker } \partial|_{\Omega_d}$, and elements in Z_d are called d -cycles. The d -th boundary group is defined as $B_d = \text{Im } \partial|_{\Omega_{d+1}}$, with elements of B_d being called d -boundary cycles (or simply d -boundaries). The resulting d -dimensional path homology group is $H_d(G, \mathbb{F}) = Z_d/B_d$.

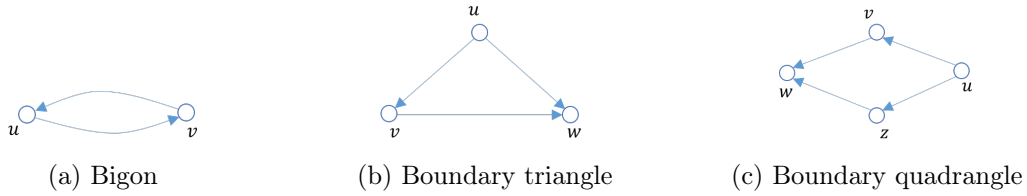


Figure 1: Examples of 1-boundaries

2.1 Examples of 1-boundaries

Below we give three examples of 1-boundaries; see Figure 1.

Bi-gon: A *bi-gon* is a 1-cycle $e_{uv} + e_{vu}$ consisting of two edges (u, v) and (v, u) from E ; see Figure 1(a). Consider the 2-path e_{uvu} . We have that its boundary is $\partial(e_{uvu}) = e_{vu} - e_{uu} + e_{uv} = e_{vu} + e_{uv}$. Since both e_{vu} and e_{uv} are allowed 1-paths, it follows that any bi-gon $e_{vu} + e_{uv}$ of G is necessarily a 1-boundary.

Boundary triangle: Consider the 1-cycle $C = e_{vw} - e_{uw} + e_{uv}$ of G (it is easy to check that $\partial C = 0$). Now consider the 2-path e_{uvw} : its boundary is then $\partial(e_{uvw}) = e_{vw} - e_{uw} + e_{uv} = C$. Note that every summand in the boundary is allowed. Thus C is a 1-boundary. We call any triangle in G isomorphic to C a *boundary triangle*. Note that a boundary triangle always has one sink and one source; see the source u and sink w in Figure 1(b). In what follows, we use $(u, w | v)$ to denote a boundary triangle where u is the source and w is the sink.

Boundary quadrangle: Consider the 1-cycle $C = e_{uv} + e_{vw} - e_{uz} - e_{zw}$ from G . It is easy to check that C is the boundary of the 2-path $e_{uvw} - e_{uzw}$, as $\partial(e_{uvw} - e_{uzw}) = e_{vw} - e_{uw} + e_{uv} - (e_{zw} - e_{uw} + e_{uz}) = e_{vw} + e_{uv} - e_{zw} - e_{uz} = C$. We call any quadrangle isomorphic to C a *boundary quadrangle*.

In the remainder of the paper, we use $R(u, v, w, z)$ to represent a quadrangle; i.e, a 1-cycle consisting of 4 edges whose *undirected version* has the form $(u, v) + (v, w) + (w, z) + (z, u)$. (Note that a quadrangle may not be a boundary quadrangle). We denote a boundary quadrangle $e_{uv} + e_{vw} - e_{uz} - e_{zw}$ by $\{u, w | v, z\}$, where u and w are the source and sink of this boundary quadrangle respectively.

3 Computing 1-dimensional path homology H_1

Note that the 1-dimensional ∂ -invariant path space $\Omega_1 = \Omega_1(G)$ is the space generated by all edges [11] because the boundary of every edge is allowed by definition.

Now consider the 1-cycle group $Z_1 \subseteq \Omega_1$; that is, Z_1 is the kernel of ∂ applied to Ω_1 . We show below that a basis of Z_1 can be computed by considering a spanning tree of the undirected version of G , which denoted by G_u . This is well known when \mathbb{F} is \mathbb{Z}_2 . It is easy to see that this spanning tree based construction also works for arbitrary field \mathbb{F} .

Specifically, let T be a rooted spanning tree of G_u with root r , and $\bar{T} := G_u \setminus T$. For every edge $e = (v_1, v_2) \in \bar{T}$, let c_e be the 1-cycle (under \mathbb{Z}_2) obtained by summing e and all edges on the paths π_1 and π_2 between v_1 and r , and v_2 and r respectively. The cycles $\{c_e, e \in \bar{T}\}$ form

a basis of 1-cycle group of G_u under \mathbb{Z}_2 coefficient. Now for every such cycle c_e in G_u , we also have a cycle in $\Omega_1(G)$ containing same edges with c_e which are assigned a coefficient 1 or -1 depending on their orientations in G . We call this 1-cycle in $\Omega_1(G)$ also c_e . Then we have the following proposition.

Proposition 3.1. *The cycles $\{c_e | e \in \bar{T}\}$ in $\Omega_1(G)$ form a basis for Z_1 under any coefficient field \mathbb{F} .*

Proof. First, it is obvious that the cycles $\{c_e | e \in \bar{T}\}$ are independent because every cycle contains a unique edge that does not exist in other cycles, which means any cycle cannot be written as a linear combination of other cycles in the set. Now what remains is to show that the cycles $\{c_e | e \in \bar{T}\}$ generate Z_1 . Consider any 1-cycle $c \neq 0$ in Z_1 with coefficients in \mathbb{F} . Observe that c must have at least one edge from \bar{T} because otherwise it will have non-zero coefficients only on edges in T whose boundary cannot be 0. Consider an edge $e_0 \in \bar{T}$ with non-zero coefficient $a_0 \in \mathbb{F}$ in c . The cycle $c' = -a_0 \cdot c_{e_0} + c$ has e_0 with zero coefficient. If c' is not 0, continue the argument again and we are guaranteed to derive a null cycle ultimately because every time we make the coefficient of an edge belonging to \bar{T} zero. This means that we have $c - a_0 c_{e_0} - \dots - a_k c_{e_k} = 0$ for some k . In other words $c = \sum_{i=0}^k a_i c_{e_i}$. It immediately follows that $\{c_e | e \in \bar{T}\}$ form a basis for Z_1 . \square

Now, we show a relation between 1-dimensional homology, cycles, bigons, triangles and quadrangles. Recall that bi-gons, boundary triangles and boundary quadrangles are specific types of 1-dimensional boundaries with two, three or four vertices, respectively; see Section 2.1. The following theorem is similar to Proposition 2.9 from [12], where the statement there is under coefficient ring \mathbb{Z} . For completeness, we include the (rather similar) proof for our case in Appendix A.

Theorem 3.1. *Let $G = (V, E)$ be a directed graph. Let Q denote the space generated by all boundary triangles, boundary quadrangles and bi-gons in G . Then we have $B_1 = Q$.*

Corollary 3.1. *The 1-dimensional path homology group satisfies that $H_1 = Z_1/Q$.*

3.1 A simple algorithm

Theorem 3.1 and Corollary 3.1 provide us a simple framework to compute H_1 . Below we only focus on the computation of the rank of H_1 ; but the algorithm can easily be modified to output a basis for H_1 as well. Later in Section 4, we will develop a more efficient and sophisticated algorithm for the 1-dimensional *persistent* path homology H_1 , which as a by-product, also gives a more efficient algorithm to compute H_1 .

In the remaining of this paper, we represent each cycle in Z_1 with a vector. Assume all edges are indexed from 1 to m as e_1, \dots, e_m where m is the number of edges. Then, each 1-cycle C is an m -dimensional vector, where $C[i] \in \mathbb{F}$ records the coefficient for edge e_i in C .

Algorithm 1 A simple first algorithm to compute rank of H_1

- 1: **procedure** COMPH1-SIMPLE(G, t)
 - 2: (Step 1): Compute rank of 1-cycle group Z_1
 - 3: (Step 2): Compute rank of 1-boundary group B_1
 - 4: (Step 2.a) Compute a *generating set* C of 1-boundary cycles that generates B_1
 - 5: (Step 2.b) From C compute a basis for B_1
 - 6: Return $rank(H_1) = rank(Z_1) - rank(B_1)$.
 - 7: **end procedure**
-

(Step 1): cycle group Z_1 . By Proposition 3.1, $\text{rank}(Z_1) = |E| - |V| + 1$ for directed graph $G = (V, E)$. The computation of the rank takes $O(1)$ time (or $O(|V|^2)$ time if we need to output a basis of it explicitly).

(Step 2): boundary group B_1 . Note that by Theorem 3.1, we can compute the set of all bigons, boundary triangles and boundary quadrangles as a *generating set* C of 1-boundary cycles (meaning that it generates the boundary group B_1) for **(Step 2.a)**. However, such a set C could have size $\Omega(n^2)$ even for a planar graph, where $n = |V|$; see Figure 2. (For a general graph, the number of boundary quadrangles could be $\Theta(n^4)$.)

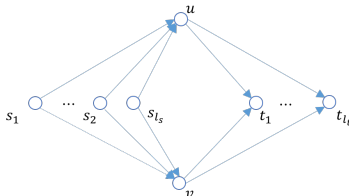


Figure 2: There are n vertices but $l_s \cdot l_t = \Theta(n^2)$ quadrangles, $l_s = \lfloor (n-2)/2 \rfloor$ and $l_t = \lceil (n-2)/2 \rceil$

To make **(Step 2.b)** efficient, we wish to have a generating set C of 1-boundary cycles with *small cardinality*. To this end, we leverage a classical result of [4] to reduce the size of C .

Given an undirected graph G where the number of multi-edges between any two vertices is constant, its *arboricity* $\mathbf{a}(G)$ is the minimum number of edge-disjoint spanning forests which G can be decomposed into [14]. An alternative definition is

$$\mathbf{a}(G) = \max_{H \text{ is a subgraph of } G} \frac{|E(H)|}{|V(H)| - 1}.$$

From this definition, it is easy to see (and well-known, see e.g. [4]) that:

Observation 3.1. *Given an undirected graph G where the number of multi-edges between any two vertices is constant:*

- (1). *If G is a planar graph, or a graph with bounded vertex degrees, then $\mathbf{a}(G) = O(1)$.*
- (2). *If G is a graph embedded on a genus g surface, then $\mathbf{a}(G) = O(g)$.*
- (3). *In general, if G does not contain self-loops, then $\mathbf{a}(G) = O(n)$.*

We will leverage some classical results from [4]. First, to represent quadrangles, we use the following *triple-list* representation [14]: a triple-list $(u, v, \{w_1, w_2, \dots, w_l\})$ means that for each i , w_i is adjacent to both u and v , where we say u' and v' are adjacent if either (u', v') or (v', u') are in E (i.e. u' and v' are adjacent when disregarding directions). Given such a triple-list $\xi = (u, v, \{w_1, w_2, \dots, w_l\})$, it is easy to see that u, w_i, v, w_j form the *consecutive vertices* of a quadrangle in the undirected version of graph G ; and we also say that the undirected quadrangle $R(u, w_i, v, w_j)$ is *covered* by this triple-list. We say that a vertex z is in a triple-list $(u, v, \{w_1, w_2, \dots, w_l\})$ if it is in the set $\{w_1, w_2, \dots, w_l\}$.

The size of a triple-list is the total number of vertices contained in it. This triple-list ξ thus represents $\Theta(l^2)$ number of undirected quadrangles in G succinctly with $\Theta(l)$ size.

Proposition 3.2 ([4]). (1) *Let G be a connected undirected graph with n vertices and m edges. There is an algorithm listing all the triangles in G in $O(\mathbf{a}(G)m)$ time.*

(2) *There is an algorithm to compute a set of triple-lists which covers all quadrangles in a connected graph G in $O(\mathbf{a}(G)m)$ time. The total size complexity of all triple-lists is $O(\mathbf{a}(G)m)$.*

Using the above result, we can have the following theorem.

Theorem 3.2. Let $G = (V, E)$ be a directed graph with n vertices and m edges. We can compute a generating set \mathcal{C} of 1-boundary cycles for \mathcal{B}_1 with cardinality $O(\mathfrak{a}(G)m)$ in time $O(\mathfrak{a}(G)m)$.

Proof. We will show that we can generate all bigons, boundary triangles and boundary quadrangles, via a generating set \mathcal{C} satisfying the requirement in the theorem.

First, note that the total number of bigons are $O(m)$ since there are m directed edges and for each edge, there is at most one bi-gon created as there is no multi-edge in G . Next, by Proposition 3.2, we have that the total number of undirected triangles is $O(\mathfrak{a}(G)m)$, which further bounds the total number of directed triangles, as well as that of the boundary triangles by $O(\mathfrak{a}(G)m)$. In particular, we enumerate all $O(\mathfrak{a}(G)m)$ undirected triangles in G in $O(\mathfrak{a}(G)m)$ time, and if the vertices form a boundary triangle, we add it to the generating set \mathcal{C} . This adds all $O(\mathfrak{a}(G)m)$ number of boundary triangles to \mathcal{C} in $O(\mathfrak{a}(G)m)$ time.

The case for quadrangles is more involved. The total number of quadrangles could be $\Theta(n^4)$ and we aim to find a subset of $O(\mathfrak{a}(G)m)$ that generate all boundary quadrangles to add to \mathcal{C} .

By Proposition 3.2, in $O(\mathfrak{a}(G)m)$ time, we can compute a list L of triple-lists with $O(\mathfrak{a}(G)m)$ total size complexity that generate all *undirected quadrangles*. Note that this also implies that $|L| = O(\mathfrak{a}(G)m)$.

Now for a triple-list $\xi_{uv} = (u, v, \{w_1, w_2, \dots, w_l\})$, we will generate three lists as follows (see Figure 3):

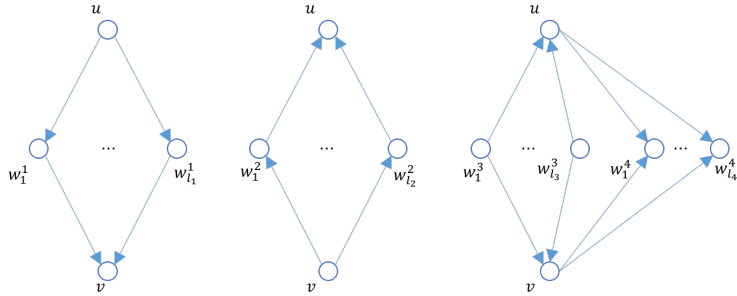


Figure 3: Three lists extracted from $\xi = (u, v, \{w_1, w_2, \dots, w_l\})$

Type-1 list: a triple-list $\xi_{uv}^{(1)} = (u, v, \{w_1^1, w_2^1, \dots, w_{l_1}^1\})$ where w_i^1 is in $\xi_{uv}^{(1)}$ if and only if $w_i^1 \in \xi_{uv}$, and both edges (u, w_i^1) and (w_i^1, v) are in E . We say that a *boundary quadrangle* can be *generated by* the type-1 list $\xi_{uv}^{(1)}$ if it is of the form $(u, v \mid w_i^1, w_j^1)$, with $i \neq j \in [1, l_1]$.

Type-2 list: a triple-list $\xi_{uv}^{(2)} = (u, v, \{w_1^2, w_2^2, \dots, w_{l_2}^2\})$ where w_i^2 is in $\xi_{uv}^{(2)}$ if any only if w_i^2 is in ξ_{uv} , and the edges (v, w_i^2) and (w_i^2, u) are in E . We say that a *boundary quadrangle* can be *generated by* the type-2 list $\xi_{uv}^{(2)}$ if it is of the form $(v, u \mid w_i^2, w_j^2)$, with $i \neq j \in [1, l_2]$.

Type-3 list: a so-called *quadruple-list* $\xi_{uv}^{(3)} = (u, v, \{w_1^3, w_2^3, \dots, w_{l_3}^3\}, \{w_1^4, w_2^4, \dots, w_{l_4}^4\})$, where each w_i^3 and w_j^4 are in ξ_{uv} , and edges (w_i^3, u) , (w_i^3, v) , (u, w_j^4) and (v, w_j^4) are in E , for $1 \leq i \leq l_3, 1 \leq j \leq l_4$. We say that a *boundary quadrangle* can be *generated by* the type-3 list $\xi_{uv}^{(3)}$ if it is of the form $(w_i^3, w_j^4 \mid u, v)$, with $i \in [1, l_3]$ and $j \in [1, l_4]$.

It is easy to see that $l_1 + l_2 + l_3 + l_4 = O(l)$. Let \widehat{L} denote all lists generated by triples in L . Note that total size complexity of \widehat{L} (which is the sum of the size of each triple-list or quadruple-list in \widehat{L}) is still $O(\mathfrak{a}(G)m)$.

Denote \mathcal{R} as the set of all boundary quadrangles in G ; note that by definition, each element in \mathcal{R} is a 1-boundary. On the other hand, each boundary quadrangle in \mathcal{R} is generated by some list in \widehat{L} . Indeed, given an arbitrary boundary quadrangle $(x, y \mid z, s)$, By Proposition 3.2, we

know that its undirected version $R(x, z, y, s)$ must be covered by some triple-list $\xi_{uv} \in L$. If $x = u$ and $y = v$, then the boundary quadrangle is then generated by the type-1 list $\xi_{uv}^{(1)}$. If $x = v$ and $y = u$, then it is generated by the type-2 list $\xi_{uv}^{(2)}$. Otherwise, by the definition of ξ_{uv} covering the undirected quadrangle $R(x, z, y, s)$, it must mean that $u = z, v = s$ or $u = s, v = z$. Thus this boundary quadrangle is generated by the type-3 list $\xi_{uv}^{(3)}$. This proves that all boundary quadrangles in \mathcal{R} are generated by the lists in the set \widehat{L} .

Finally, we will add boundary quadrangles to \mathbf{C} as follows: We inspect each list in \widehat{L} .

Case 1 : If it is a type-1 list, say of the form $\xi_{uv}^{(1)} = (u, v, \{w_1^1, w_2^1, \dots, w_{l_1}^1\})$, we add $l_1 - 1$ number of boundary quadrangles of the form $(u, v \mid w_i^1, w_{i+1}^1)$ to \mathbf{C} for each $i \in [2, l_1]$.

Case 2 : If it is a type-2 list of the form $\xi_{uv}^{(2)} = (u, v, \{w_1^2, w_2^2, \dots, w_{l_2}^2\})$, we then add $l_2 - 1$ number of boundary quadrangles of the form $(v, u \mid w_i^2, w_{i+1}^2)$ to \mathbf{C} , for each $i \in [2, l_2]$.

Case 3 : If it is a type-3 list of the form $\xi_{uv}^{(3)} = (u, v, \{w_1^3, w_2^3, \dots, w_{l_3}^3\}, \{w_1^4, w_2^4, \dots, w_{l_4}^4\})$, then we add $l_3 + l_4$ number of boundary quadrangles of the form $(w_1^3, w_i^4 \mid u, v)$ or $(w_j^3, w_1^4 \mid u, v)$ into \mathbf{C} , for each $i \in [1, l_4]$ and $j \in [1, l_3]$.

Note that for each case above, the subset of quadrangles we add to \mathbf{C} can generate all the boundary quadrangles generated by the corresponding list $\xi_{uv}^{(k)}$ for $k = 1, 2$, or 3 . Indeed, for (Case 1): each boundary quadrangle $(u, v \mid w_i^1, w_j^1)$ generated by $\xi_{uv}^{(1)}$ can be written as the linear combination of $(u, v \mid w_1^1, w_j^1)$ and $(u, v \mid w_i^1, w_1^1)$, both of which are added to \mathbf{C} . (Case 2) can be argued in a symmetric manner. For (Case 3), consider a boundary quadrangle $(w_j^3, w_i^4 \mid u, v)$ generated by $\xi_{uv}^{(3)}$. It can be written as the combination of $(w_j^3, w_1^4 \mid u, v)$, $(w_1^3, w_i^4 \mid u, v)$ and $(w_1^3, w_i^4 \mid u, v)$, all of which on the righthand side are added to \mathbf{C} .

Hence in summary, the set of quadrangles we add to \mathbf{C} will generate all boundary quadrangles \mathcal{R} . Furthermore, note that in each case, the number of quadrangles we add to \mathbf{C} is linear in the size of the list from \widehat{L} being considered. Hence the total number of boundary quadrangles ever added to \mathbf{C} is bounded by the total size of \widehat{L} which is further bounded by $O(\mathfrak{a}(G)m)$. Putting everything together, the theorem then follows. \square

It then follows from Theorem 3.1 that (Step 2.a) can be implemented in $O(\mathfrak{a}(G)m)$ time, producing a generating set of cardinality $O(\mathfrak{a}(G)m)$. Finally, representing each boundary cycle in \mathbf{C} as a vector of dimension $m = |E|$, we can then compute the rank of cycles in \mathbf{C} in $O(|\mathbf{C}|m^{\omega-1}) = O(\mathfrak{a}(G)m^\omega)$, where $\omega < 2.373$ is the exponent for matrix multiplication [3].

Putting everything together, we have that

Theorem 3.3. *Given a directed graph $G = (V, E)$ with $n = |V|$ and $m = |E|$, Algorithm 1 computes the rank of the 1-dimensional path homology group \mathbf{H}_1 in $O(\mathfrak{a}(G)m^\omega)$ time. The algorithm can be extended to compute a basis for \mathbf{H}_1 with the same time complexity.*

For example, by Observation 3.1, if G is a planar graph, then we can compute \mathbf{H}_1 in $O(n^\omega)$. For a graph G embedded on a genus g surface, \mathbf{H}_1 can be computed in $O(gm^\omega)$ time. In contrast, we note that the algorithm of [6] takes $O(n^5)$ time for planar graphs.

4 Computing persistent path homology \mathbf{H}_1

The concept of arboricity used in the previous section does not consider edge directions. Indeed, our algorithm to compute a generating set \mathbf{C} as given in the proof of Theorem 3.2 first computes a (succinct) representation of all quadrangles, whether they contribute to boundary quadrangles or not. On the other hand, as Figure 4 illustrates, a graph G can have no boundary quadrangle despite the fact that the graph is dense (with $\Theta(n^2)$ edges and thus $\mathfrak{a}(G) = \Theta(n)$ arboricity).

Another way to view this is that the example has no allowed 2-path, and thus no ∂ -invariant 2-paths and consequently no 1-boundary cycles. Our algorithm will be more efficient if it can also respect the number of allowed elementary 2-paths.

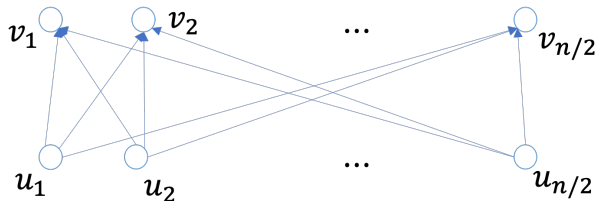


Figure 4: A dense graph with no boundary quadrangle

In fact, a more standard and natural way to compute a basis for the 1-boundary group proceeds by taking the boundary of ∂ -invariant 2-paths. The complication is that unlike in the simplicial homology case, it is not immediately evident how to compute a basis for Ω_2 (the space of ∂ -invariant 2-paths). Nevertheless, Chowdhury and Mémoli presented an elegant algorithm to show that a basis for B_1 (and H_1) can still be computed using careful column-based matrix reductions [6]. The time complexity of their algorithm is $O((\sum_{(u,v) \in E} (d_{in}(u) + d_{out}(v)))mn^2)$ which depends on the number of elementary 2-paths ³.

In this section, we present an algorithm that can take advantage of both of the previous approaches (the algorithm of [6] and Algorithm 1). Similar to [6], we will now consider the persistent path homology setting, where we will add directed edges in G one by one incrementally. Hence our algorithm can compute the *persistent* H_1 w.r.t. a filtration. However different from [6], instead of reducing a matrix with columns corresponding to all elementary allowed 2-paths, we will follow a similar idea as in Algorithm 1 and add a generating set of boundary cycles each time we consider a new directed edge.

4.1 Persistent path homology

We now introduce the definition of the persistent path homology [6]. The *persistent vector space* is a family of vector spaces together with linear maps $\{U^\delta \xrightarrow{\mu_{\delta, \delta'}} U_{\delta \leq \delta' \in \mathbb{R}}^{\delta'}\}$ so that: (1) $\mu_{\delta, \delta}$ is the identity for every $\delta \in \mathbb{R}$; and (2) $\mu_{\delta, \delta''} = \mu_{\delta, \delta'} \circ \mu_{\delta', \delta''}$ for each $\delta \leq \delta' \leq \delta'' \in \mathbb{R}$.

Let $G = (V, E, w)$ be a weighted directed graph where V is the vertex set, E is the edge set, and w is the weight function $w : E \rightarrow \mathbb{R}^+$. For every $\delta \in \mathbb{R}^+$, a directed graph G^δ can be constructed as $G^\delta = (V^\delta = V, E^\delta = \{e \in E : w(e) \leq \delta\})$. This gives rise to a filtration of graphs $\{G^\delta \hookrightarrow G^{\delta'}\}_{\delta \leq \delta' \in \mathbb{R}}$ using the natural inclusion map $i_{\delta, \delta'} : G^\delta \hookrightarrow G^{\delta'}$.

Definition 4.1. [6] *The 1-dimensional persistent path homology of a weighted directed graph $G = (V, E, w)$ is defined as the persistent vector space $\mathbb{H}_1 := \{H_1(G^\delta) \xrightarrow{i_{\delta, \delta'}} H_1(G^{\delta'})\}_{\delta \leq \delta' \in \mathbb{R}}$. The 1-dimensional path persistence diagram $Dg(G)$ of G is the persistence diagram of \mathbb{H}_1 .*

To compute the path homology $H_1(G)$ of an unweighted directed graph $G = (V, E)$, we can order edges in E arbitrarily with the index of an edge in this order being its weight. The rank of $H_1(G)$ can then be retrieved from the 1-dimensional persistent homology group induced by this filtration by considering only those homology classes that “never die”.

³The time complexity given in the paper [6] assumes that the input directed graph is complete, and takes $O(n^9)$ to compute H_1 . However, a more refined analysis of their time complexity shows that it can be improved to $O((\sum_{(u,v) \in E} d_{in}(u) + d_{out}(v))mn^2)$.

(Case-B): The endpoints u and v are already in the same connected component in $G^{(s-1)}$. After adding this edge e_s , new cycles are created in $G^{(s)}$. Hence e_s is *positive* in this case (as it creates an element in \mathbf{Z}_1 ; although different from the standard simplicial homology, it may not necessarily create an element in \mathbf{H}_1 as we will see later).

Whether e_s is positive or negative can be easily determined by performing two Find operations in the union-find data structure representing T_{s-1} . A $\text{Union}(u, v)$ operation is performed to update T_{s-1} to T_s if e_s is negative.

We now describe how to handle (Case-B). After adding edge e_s , multiple cycles containing e_s can be created in $G^{(s)}$. Nevertheless, by Proposition 3.1, the dimension of \mathbf{Z}_1 increases only by 1. On the other hand, the addition of e_s may create new boundary cycles. Interestingly, it could increase the rank of \mathbf{B}_1 by more than 1. See Figure 5 for an example where $\text{rank}(\mathbf{B}_1)$ increases by 3; and note that this number can be made arbitrarily large.

As mentioned earlier, in this case, we wish to compute a set of generating boundary cycles \mathbf{C}_s such that $B \cup \mathbf{C}_s$ contains a basis for $\mathbf{B}_1(G^{(s)})$.

Similar to Algorithm 1, using Theorem 3.1, we choose some bigons, boundary triangles and boundary quadrangles and add them to \mathbf{C}_s . In particular, since \mathbf{C}_s only accounts for the newly created boundary cycles, we only need to consider bigons, boundary triangles and boundary quadrangles that contain e_s . We now describe the construction of \mathbf{C}_s , which is initialized to be \emptyset .

(i) *Bigons*. At most one bigon can be created after adding e_s (namely, the one that contains e_s). We add it to \mathbf{C}_s if this bigon exists.

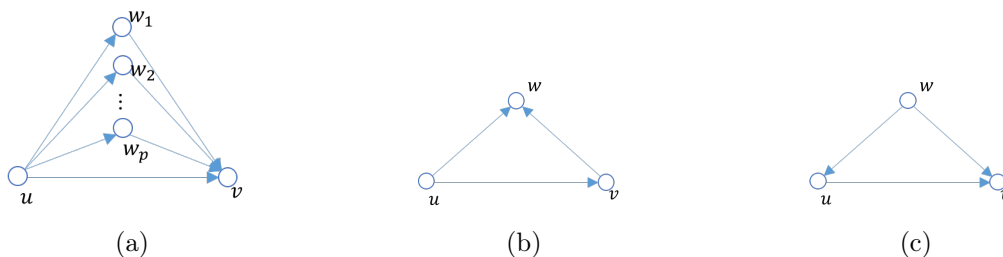


Figure 6: Three types of boundary triangles incident to $e_s = (u, v)$.

(ii) *Boundary triangles*. There could be three types of newly created boundary triangles containing $e_s = (u, v)$. The first case is when u is the source and v is the sink; see Figure 6(a). In this case multiple 2-paths may exist from u to v , $e_{uw_1v}, e_{uw_2v}, \dots, e_{uw_pv}$, forming multiple boundary triangles of this type containing e_s . However, we only need to add *one* triangle of them into \mathbf{C}_s , say $(u, v | w_1)$ since every other triangle $(u, v | w_j)$ can be written as a linear combination of $(u, v | w_1)$ and an existing boundary quadrangle $(u, v | w_1, w_j)$ in $G^{(s-1)}$.

For the second case (see Figure 6(b)) where u is the source but v is not the sink, we include all such boundary triangles to \mathbf{C}_s . We also add all boundary triangles of the last type in which v is the sink but u is not the source to \mathbf{C}_s ; see Figure 6(c). It is easy to see that $\mathbf{C}_s \cup B$ can generate all new boundary triangles containing $e_s = (u, v)$.

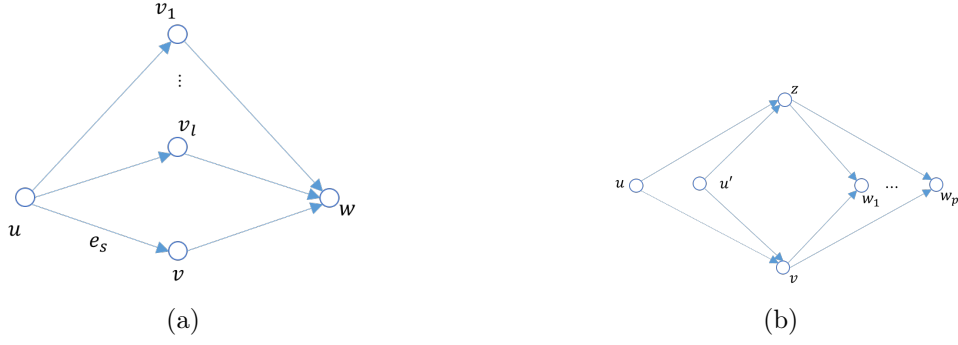


Figure 7: (a) Examples of new boundary quadrangles with u being the source. (b) Not all boundary quadrangles in M will be added to the generating set C_s .

(iii) *Boundary quadrangles.* Given an edge $e_s = (u, v)$, there are two types of the boundary quadrangles incident to it: one has u as the source; the other has v as the sink. We focus on the first case; see Figure 7(a). The second case can be handled symmetrically.

In particular, we will first compute a set M and then select a subset of quadrangles from M for adding to C_s .

Specifically, take any successor w of v , that is, there is an edge $(v, w) \in G^{(s-1)}$ forming an allowed 2-path e_{uvw} in $G^{(s)}$. Before introducing the edge e_s , there may be multiple allowed 2-paths $e_{uv_1w}, e_{uv_2w}, \dots, e_{uv_lw}$ in $G^{(s-1)}$; see Figure 7 (a). For each such 2-path e_{uv_kw} , $1 \leq k \leq l$, a new boundary quadrangle $(u, w | v, v_k)$ containing $e_s = (u, v)$ will be created. However, among all such 2-paths $e_{uv_1w}, \dots, e_{uv_lw}$, we will pick just one 2-path, say e_{uv_1w} and only add the quadrangle $(u, w | v, v_1)$ formed by e_{uvw} and e_{uv_1w} to M . Observe that any other boundary quadrangle containing 2-path e_{uvw} , say $(u, w | v, v_k)$, can be written as a linear combination of the quadrangle $(u, w | v, v_1)$ and boundary quadrangle $(u, w | v_k, v_1)$ which is already in $G^{(s-1)}$ (and in the span of B which is a basis for $B_1(G^{(s-1)})$). In other words, $(u, w | v, v_1) \cup B$ generates any other boundary quadrangle containing 2-path e_{uvw} .

We perform this for each successor w of v . Hence this step adds at most $d_{out}^{G^{(s-1)}}(v)$ number of boundary quadrangles to the set M .

Not all quadrangles in M will be added to C_s . In particular, suppose we have p quadrangles $A = \{(u, w_j | v, z) : 1 \leq j \leq p\} \subseteq M$ incident to the newly inserted edge $e_s = (u, v)$ as well as another vertex z , i.e. there are edges $(u, z), (w_j, z)$ and (v, w_j) , $1 \leq j \leq p$; see Figure 7 (b). If there does not exist any other vertex u' such that edges $(u', z), (u', v) \in G^{(s-1)}$, then we add *all* quadrangles in A to C_s . If this is not the case, let u' be another vertex such that (u', z) and (u', v) are already in $G^{(s-1)}$; see Figure 7 (b). In this case, we only add *one* quadrangle from set A , say, $(u, w_1 | v, z)$ to the generating set C_s .

It is easy to check that any other quadrangle $(u, w_j | v, z)$, $1 < j \leq p$, can be written as the combination of $(u, w_1 | v, z)$, $(u', w_1 | v, z)$ and $(u', w_j | v, z)$. As the latter two quadrangles are boundary quadrangles from $G^{(s-1)}$, they can already be generated by B . The entire process takes time $O(|M|) = O(d_{out}^{G^{(s-1)}}(v))$. It is also easy to see that $B \cup C_s$ can generate any boundary quadrangle containing $e_s = (u, v)$ and with u being its source.

The case when v is the sink of a boundary quadrangle is handled symmetrically in time $O(d_{in}^{G^{(s-1)}}(u))$. Hence the total time to compute a generating set C_s is $O(d_{in}^{G^{(s-1)}}(u) + d_{out}^{G^{(s-1)}}(v))$ when inserting a single edge $e_s = (u, v)$.

4.2.2 Procedure FINDPAIRS

Given the generating set C_s and the previous basis B for $B_1(G^{(s-1)})$, we know that $C_s \cup B$ generate the new boundary group $B_1(G^{(s)})$. We now extract a basis B_{new} for $B_1(G^{(s)})$ from

$B \cup \mathcal{C}_s$.

We represent each 1-cycle γ by an m -dimensional vector, also denoted by γ , so that $\gamma = \sum_{i=1}^m \gamma[i]e_i$. (Note that e_1, \dots, e_m are sorted according to their filtration order.) A set of k cycles can now be viewed as a $m \times k$ matrix, where the i -th column corresponds to the vector representation of the i -th cycle.

Thus columns in the matrix B correspond to cycles in an existing basis for $\mathbf{B}_1(G^{(s-1)})$, and are already linearly independent. Our goal is now to compute a basis of the form $[B \mid B']$ for the matrix $[B \mid \mathcal{C}_s]$, and the columns in B and B' form a new basis B_{new} for $\mathbf{B}_1(G^{(s)})$.

To do so, we follow the standard persistence algorithm which would also output persistence pairings for \mathbf{H}_1 . Specifically, Let $low(j)$ be the row index of the last non-zero entry in column j in a matrix A . A matrix A is in *reduced form* if the $low(j)$ in each column j is unique. We compute persistent pairs by always maintaining the basis in reduced form [7]. Here assume that B is already in reduced form. We then perform standard column reduction to convert $[B \mid \mathcal{C}_s]$ into reduced form $[B \mid R]$. For each non-zero column $R[j]$ in R , let $k = low(j)$ be the index of its lowest non-zero entry. Let e_k be the edge corresponding to this entry in the cycle corresponding to column $R[j]$. This means that the cycle corresponding to $R[j]$ is created when e_k introduced, but killed when introducing e_s , since currently it is a boundary. Then we add the persistence pairing $(w(e_k), w(e_s))$ to the output persistence diagram Dg_1G for the 1-dimensional path homology.

The collection of non-zero columns in R gives rise to B' . Afterwards, we update B to be $B \cup B'$, and proceed to process the next edge e_{s+1} .

4.3 Analysis of Algorithm 2

Correctness. Notice that the invariant that B is a basis for $G^{(s)}$ at the end of the for-loop (line-7 of Algorithm 2) is maintained. Furthermore, B is always in reduced form which is maintained via left-to-right column additions only. Hence the algorithm computes the 1-dimensional persistent path homology correctly [7].

Time complexity analysis. The remainder of this section is devoted to determining the time complexity of Algorithm 2. Specifically, we first show the following theorem.

Theorem 4.1. *Across all stages $s \in [1, m]$, the total cardinality of the generating set $\mathcal{C} = \cup_s \mathcal{C}_s$ is $O(\min\{\mathbf{a}(G)m, \sum_{(u,v) \in E} (d_{in}(u) + d_{out}(v))\})$. The total time taken by procedure `NEWBASIS`(s) for all $s \in [1, m]$ is $O(m + \sum_{(u,v) \in E} (d_{in}(u) + d_{out}(v)))$.*

Proof. We will count separately the number of bigons, boundary triangles, and boundary quadrangles added to any \mathcal{C}_s . Set $r = \min\{\mathbf{a}(G)m, \sum_{(u,v) \in E} (d_{in}(u) + d_{out}(v))\}$.

(i) *Bigons:* First, it is easy to see that for each edge $e_s = (u, v)$ with $s \in [1, m]$, at most one bigon (incident to e_s) is added. Besides, if $d_{out}(v) = 0$, there is no bigon incident to e_s . Hence the total number ever added to \mathcal{C} is $O(\min\{m, \sum_{(u,v) \in E} (d_{out}(v))\}) = O(r)$ and it takes $O(m)$ time to compute them.

(ii) *Boundary triangles:* For boundary triangles, we know from Proposition 3.2 that there are altogether $O(\mathbf{a}(G)m)$ triangles (thus at most $O(\mathbf{a}(G)m)$ boundary triangles) in a graph G and they can all be enumerated in $O(\mathbf{a}(G)m)$ time. Obviously, the number of boundary triangles ever added to \mathcal{C} is at most $O(\mathbf{a}(G)m)$.

We now argue that the number of boundary triangles added to \mathcal{C} is also bounded by $O(\sum_{(u,v) \in E} (d_{in}(u) + d_{out}(v)))$. Note that, for every 2-path, at most one boundary triangle is added to the set. Since the number of 2-paths is indeed $\Theta(\sum_{(u,v) \in E} (d_{in}(u) + d_{out}(v)))$, the number of triangles we add is $O(\sum_{(u,v) \in E} (d_{in}(u) + d_{out}(v)))$. Recall that there are three cases for boundary triangles added; see Figure 6. The time spent for the first case for every s is $O(1)$ by recording any 2-path e_{uvw} , and $O(d_{in}(u) + d_{out}(v))$ for the last two cases. Thus the total time spent at adding

boundary triangles incident to e_s and identifying triangles to be added to C_s for all $s \in [1, m]$ takes $O(m + \sum_{(u,v) \in E} (d_{in}(u) + d_{out}(v)))$ time.

(iii) *Boundary quadrangles*: The situation here is somewhat opposite to that of the boundary triangles: Specifically, it is easy to see that this step accesses at most $O(d_{in}(u) + d_{out}(v))$ boundary quadrangles when handling edge $e_s = (u, v)$. Hence the number of boundary quadrangles it can add to C_s is at most $O(d_{in}(u) + d_{out}(v))$. The total number of boundary quadrangles ever added to C is thus bounded by $O(\sum_{(u,v) \in E} (d_{in}(u) + d_{out}(v)))$.

We now prove that the number of boundary quadrangles ever added to C is also bounded by $O(a(G)m)$. We use the existence of a succinct representation of all quadrangles as specified in Proposition 3.2 to help us argue this upper bound. Notice that our algorithm **does not** compute this representation. It is only used to provide this complexity analysis.

Specifically, by Proposition 3.2, we can compute a list L of triple-lists with $O(a(G)m)$ total size complexity, which generates all undirected quadrangles. Following the proof of Theorem 3.2, we can further refine this list, where each triple-list $\xi \in L$ further gives rise to three lists that are of type-1, 2, or 3. Let \widehat{L} denote this refinement of L , consisting of lists of type-1, 2 or 3. From the proof of Theorem 3.2, we know that the total size complexity for all lists in \widehat{L} is still $O(a(G)m)$. This also implies that the cardinality of \widehat{L} is bounded by $|\widehat{L}| = O(a(G)m)$.

We now denote by \mathcal{R} the set of all boundary quadrangles ever added to $C = \cup_s C_s$ by Algorithm 2. Furthermore, let

$$\mathcal{P} := \{(\xi, w) \mid \xi \in \widehat{L}, w \in \xi\}.$$

Below we show that we can find an injective map $\pi : \mathcal{R} \rightarrow \mathcal{P}$. But first, note that $|\mathcal{P}|$ is proportional to the total size complexity of \widehat{L} and thus is bounded by $O(a(G)m)$.

We now establish the injective map $\pi : \mathcal{R} \rightarrow \mathcal{P}$. Specifically, we process each boundary quadrangle *in the order* that they are added to C . Consider a boundary quadrangle $R = R(u, v, w, z)$ added to C_s while processing edge $e_s = (u, v)$. There are two cases: The first is that R is of the form $(u, w \mid v, z)$ in which u is the source of this quadrangle. The second is that it has the form $(w, v \mid u, z)$ in which v is the sink. We describe the map $\pi(R)$ for the first case, and the second one can be analyzed symmetrically.

By construction of L , there is at least one triple-list $\xi \in L$ covering $R = (u, w \mid v, z)$. There are three possibilities:

(Case-a): The triple-list ξ is of the form $\xi = \xi_{uw} = (u, w, \{\dots\})$. In this case, the boundary quadrangle $R = (u, w \mid v, z)$ is in a type-1 list $\xi_{uw}^{(1)} = (u, w, S) \in \widehat{L}$, and both $v, z \in S$. We now claim that the pair $(\xi_{uw}^{(1)}, v) \in \mathcal{P}$ has not yet been mapped (i.e, there is no $R' \in C$ with $\pi(R') = (\xi_{uw}^{(1)}, v)$ yet), and we can thus set $\pi(R) = (\xi_{uw}^{(1)}, v) \in \mathcal{P}$. Suppose on the contrary there already exists $R' \in C$ that we processed earlier than R with $\pi(R') = (\xi_{uw}^{(1)}, v)$. In that case, $R' = (u, w \mid v, z')$ must contain the 2-path e_{uvw} as well. Since R' is processed earlier than R , and edge $e_s = (u, v)$ is the most recent edge added, R' must be added when we process e_s as well (as R' contains e_s). However, Algorithm 2 in this case only adds *one* quadrangle containing the 2-path e_{uvw} , meaning that R' cannot exist (as otherwise, we would not have added R to C_s ; recall Figure 7 (a)). Hence, the map π so far remains injective.

(Case-b): The triple-list ξ is of the form $\xi = \xi_{wu} = (w, u, \{\dots\})$. In this case, this quadrangle is covered by the type-2 list $\xi_{wu}^{(2)} \in \widehat{L}$. We handle this in a manner symmetric to (Case-a) and map $\pi(R) = (\xi_{wu}^{(2)}, v)$.

(Case-c): The last case is that R is generated by triple-list ξ of the form $\xi_{vz} = (v, z, \{\dots\})$. In this case, the quadrangle $R = (u, w \mid v, z)$ will be covered by the type-3 list $\xi_{vz}^{(3)} = (v, z, S_1, S_2)$ with $u \in S_1$ and $w \in S_2$; see Figure 8. We now argue that at least one of $(\xi_{vz}^{(3)}, u)$ and $(\xi_{vz}^{(3)}, w)$ has *not* been mapped under π yet.

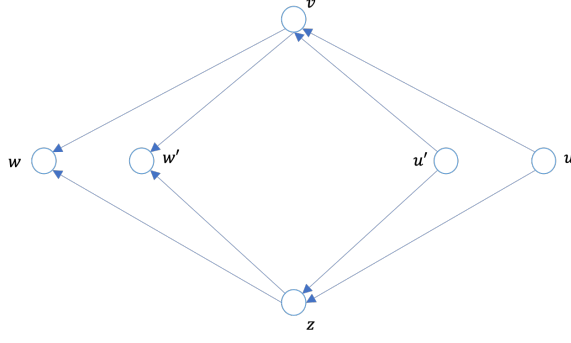


Figure 8: At least one of $(\xi_{vz}^{(3)}, u)$ and $(\xi_{vz}^{(3)}, w)$ has not been mapped yet.

Suppose this is not the case and we already have both $\pi(Q_1) = (\xi_{vz}^{(3)}, u)$ and $\pi(Q_2) = (\xi_{vz}^{(3)}, w)$. Then Q_1 is necessarily of the form $(u, w' \mid v, z)$ and Q_2 is of the form $(u', w \mid v, z)$; and both Q_1 and Q_2 are processed before R . See Figure 8. Furthermore, Q_1 is only added when we process edge e_s . However, in this case, once Q_1 is added, Algorithm 2 will not add further quadrangle containing edges (u, v) and (u, z) (recall the handling of Figure 7 (b)). Hence R cannot be added to \mathcal{C}_s in this case.

In other words, it cannot be that both Q_1 and Q_2 already exist, and hence we can set $\pi(R)$ to be one of $(\xi_{vz}^{(3)}, u)$ and $(\xi_{vz}^{(3)}, w)$ that is not yet mapped. Consequently, the map π we construct remains injective.

We process all quadrangles in \mathcal{C} in order. The final $\pi : \mathcal{R} \rightarrow \mathcal{P}$ is injective, meaning that $|\mathcal{R}| \leq |\mathcal{P}|$ and thus $|\mathcal{R}| = O(\mathfrak{a}(G)m)$.

Putting everything together, we have that the total number of boundary quadrangles added to \mathcal{C} is bounded by $O(\min\{\mathfrak{a}(G)m, \sum_{(u,v) \in E} (d_{in}(u) + d_{out}(v))\})$.

Finally, Algorithm 2 spends $O(m + \sum_{(u,v) \in E} (d_{in}(u) + d_{out}(v)))$ time to handle both cases in Figure 7. The theorem then follows. \square

We now prove our main result, Theorem 1.1. In particular, below we first show that Algorithm 2 takes $O(rm^2)$ time to compute the 1-dimensional *persistent* path homology, where

$$r = \min\{\mathfrak{a}(G)m, \sum_{(u,v) \in E} (d_{in}(u) + d_{out}(v))\}.$$

We then describe how to improve the time complexity to $O(rm^{\omega-1})$ to establish Theorem 1.1.

Specifically, by using a union-find data structure to maintain a spanning forest for $G^{(s)}$, it takes $O(m\alpha(n))$ time, where $\alpha(\cdot)$ is the inverse Ackermann function, to check whether each edge e_s is negative or positive (forming a cycle or not). As explained in the algorithm, if it is negative, then nothing needs to be done. If it is positive, then we need to compute a generating set as well as find new basis for the boundary group and compute persistence.

By Theorem 4.1, the total time complexity spent on all executions of line 5 of Algorithm 2 is $O(m + \sum_{(u,v) \in E} (d_{in}(u) + d_{out}(v)))$. We now argue that this value is bounded by $O(rm)$. This clearly holds if $r = \sum_{(u,v) \in E} (d_{in}(u) + d_{out}(v))$. If on the other hand $r = \mathfrak{a}(G)m$, then $r = \Omega(m)$ and since $\sum_{(u,v) \in E} (d_{in}(u) + d_{out}(v)) = O(mn)$, we have that

$$m + \sum_{(u,v) \in E} (d_{in}(u) + d_{out}(v)) = O(r) + O(mn) = O(rm).$$

Next we bound the total time taken by all executions of line 6 of Algorithm 2 (i.e, on calling procedure $\text{FINDPAIRS}(s)$ for all $s \in [1, m]$). Note that at the s -th stage, we need to reduce $|\mathcal{C}_s|$ number of columns in a matrix of the form $[B \mid \mathcal{C}_s]$, each of which is of length m . Furthermore,

since when reducing a specific column in a left-to-right manner, the number of non-zero columns to its left is bounded by the size of $\text{rank}(\mathbf{B}_1(G^{(s)})) = O(m)$, each column-reduction takes $O(m^2)$ time. As $|\mathbf{C}| = \sum_s |\mathbf{C}_s| = O(r)$ by Theorem 4.1, procedure $\text{FINDPAIRS}(s)$ for all $s \in [1, m]$ takes $O(rm^2)$ time. It follows that Algorithm 2 takes time $O(rm + rm^2) = O(rm^2)$.

Improving the time complexity. We see that the dominating term for the time complexity of Algorithm 2 is the time spent on procedure $\text{FINDPAIRS}(s)$ for all $s \in [1, m]$. To this end, instead of reducing the columns for each $s = 1, \dots, m$, we compute the earliest basis from the matrix $[\mathbf{C}_1 \mid \mathbf{C}_s \mid \dots \mid \mathbf{C}_m]$ by the algorithm in [17]. Here the earliest basis of a matrix A with rank r means the set of columns $B_{opt} = \{a_{i_1}, \dots, a_{i_r}\}$ if the column indices $\{i_1, \dots, i_r\}$ are the lexicographically smallest index set such that the corresponding columns of A have full rank. Since $|\cup_s \mathbf{C}_s| = O(r)$ and the number of independent columns is $O(m)$, this can be done in $O(\binom{r}{m} m^\omega) = O(rm^{\omega-1})$ time. This finishes the proof of Theorem 1.1.

Remark: 1 We note that neither term in $r = \min\{\mathbf{a}(G)m, \sum_{(u,v) \in E} (d_{in}(u) + d_{out}(v))\}$ always dominates. In particular, it is easy to find examples where one term is significantly smaller (asymptotically) than the other. For example, for any planar graph G , $\mathbf{a}(G)m = O(n)$. However, it is easy to have a planar graph where the second term $\sum_{(u,v) \in E} (d_{in}(u) + d_{out}(v)) = \Omega(n^2)$; see e.g, Figure 2.

On the other hand, it is also easy to have a graph G where $\sum_{(u,v) \in E} (d_{in}(u) + d_{out}(v)) = O(1)$ yet $\mathbf{a}(G)m = \Theta(n^3)$. Indeed, consider the bipartite graph in Figure 4, where for each edge $(u, v) \in E$, $d_{in}(u) + d_{out}(v) = 0$. However, this graph has $\mathbf{a}(G) = \Theta(n)$, $m = \Theta(n^2)$ and thus $\mathbf{a}(G)m = \Theta(n^3)$.

Remark: 2: We note that the time complexity of the algorithm proposed by Chowdhury and Mémoli in [6] to compute the $(d - 1)$ -dimensional persistence path homology takes $O(n^{3+3d})$ time. However, for the case $d = 2$, a more refined analysis shows that in fact, their algorithm takes only $O((\sum_{(u,v) \in E} (d_{in}(u) + d_{out}(v)))mn^2)$ time.

Compared with our algorithm, which takes time $O(rm^{\omega-1})$ with $r = \min\{\mathbf{a}(G)m, \sum_{(u,v) \in E} (d_{in}(u) + d_{out}(v))\}$ and $\omega < 2.373$, observe that our algorithm can be significantly faster (when $\mathbf{a}(G)m$ is much smaller than $\sum_{(u,v) \in E} (d_{in}(u) + d_{out}(v))$). For example, for planar graphs, our algorithm takes $O(n^\omega)$ time, whereas the algorithm of [6] takes $O(n^5)$ time.

5 Applications

We first show in Section 5.1 that our new algorithm can be extended to compute a minimal 1-dimensional path homology basis. We then show in Section 5.2 some preliminary experimental results for our algorithms, including showing the efficiency of our algorithm compared to the previous best algorithm over several datasets.

5.1 Annotations and minimum 1-dimensional (path) homology basis

Our algorithm can also compute a (1-dimensional) minimal homology basis for a directed graph $G = (V, E)$. In particular, let $g = \text{rank}(\mathbf{H}_1)$, and assume that $G = (V, E)$ is equipped with positive edge weights $w : E \rightarrow \mathbb{R}^+$. Given any 1-cycle $\gamma = \sum c_i e_i$, for each $i \in [1, m]$ set $\hat{c}_i = 1$ if $c_i \neq 0$; and $\hat{c}_i = 0$ otherwise. Then the length of γ , $\mu(\gamma)$, equals $\mu(\gamma) = \sum_i \hat{c}_i w(e_i)$.

Now abusing the notations slightly, we say that a set of g 1-cycles $\{\gamma_1, \dots, \gamma_g\}$ forms a 1-dimensional homology basis if the homology classes they represent, $\{[\gamma_1], \dots, [\gamma_g]\}$, forms a basis for $\mathbf{H}_1(G)$. The total length of this homology basis equals the total lengths of all cycles involved, i.e. $\sum_{i=1}^g \mu(\gamma_i)$.

Definition 5.1. Given a weighted directed graph $G = (V, E)$, let g be the rank of 1-dimensional homology group $\mathbf{H}_1(G)$. Let $\mu : \mathbf{Z}_1 \rightarrow \mathbb{R}^+ \cup \{0\}$ be the length of each cycle $C \in \mathbf{Z}_1$. A homology basis $\gamma_1, \dots, \gamma_g$ is called minimal if $\sum_{i=1}^g \mu(\gamma_i)$ is minimal among all bases of \mathbf{H}_1 .

Annotation To this end, we first compute the so-called annotations of cycles to represent its homology class [1]. Then we use annotation to compute a minimal homology basis. In particular, for every 1-chain $\gamma \in \Omega_1$, we assign γ a g -bit vector $\alpha(\gamma)$, called the *annotation of γ* , such that any two cycles C and C' are homologous if and only if their annotations $\alpha(C)$, $\alpha(C')$ are the same. As before, set $r = \min\{\mathbf{a}(G)m, \sum_{(u,v) \in E} (d_{in}(u) + d_{out}(v))\}$.

We compute the annotation according to [1]. First we compute the annotation for every edge. We construct a cycle basis Z in which any cycle can be expressed in simple and efficient terms. Note that as in the previous section, Algorithm 2 can not only compute a basis for $\mathbf{H}_1(G)$, it can in fact partition edges into negative edge set and positive edge set, in which all negative edges $E(T)$ form a spanning tree T , while every positive edge $e \in \hat{E} = E \setminus E(T)$ can create a new cycle together with T , denoted as $\gamma(T, e)$. Note that $\gamma(T, e)$ can be written as a m -bit vector. According to Proposition 3.1, all such cycle form a cycle basis Z . For every tree edge $e \in E(T)$, let $\gamma(T, e)$ be a m -bit vector where every element is 0. It has been proved in [1] that for any cycle $C = \sum_i c_i e_i$ where c_i is the coefficient of e_i in C , it holds that $C = \sum_i c_i \gamma(T, e_i)$. Note that Algorithm 2 indeed computes a boundary basis B for $\mathbf{B}_1(G)$ and a homology basis H for $\mathbf{H}_1(G)$, such that $B \cup H$ forms another cycle basis \hat{Z} for the cycle-group $\mathbf{Z}_1(G)$ where $rank(\hat{Z}) = rank(Z) = m - n + 1$. Thus for every cycle $\gamma(T, e)$, we can solve a linear system $\hat{Z}x = \gamma(T, e)$. As a result, x will be a $(m - n + 1) \times 1$ vector. We assign last $g = rank(\mathbf{H}_1)$ -bits as the annotation $\alpha(e)$ of e . We can solve for the annotation for all edges in $O(m^\omega)$ time where m is the number of edges. Combined with time needed to compute the homology basis H , we conclude that computing the annotations of all edges costs $O(\min\{\mathbf{a}(G)m, \sum_{(u,v) \in E} (d_{in}(u) + d_{out}(v))\}m^{\omega-1} + m^\omega)$ time.

After computing the annotation for every edge, $\alpha(e)$ for every edge e , for every 1-cycle $C = \sum_i c_i e_i$ where c_i is the coefficients for the edge e_i , its annotation can be computed as $\alpha(C) = \sum_i c_i \alpha(e_i)$.

Minimal homology basis We now compute a minimal homology basis. Using the results in [18], we observe that there is a collection of cycles, called Horton family, that includes a minimal homology basis. It is known from [15] that the cardinality of the Horton family is $O(nm)$. Using same steps as in [18], replacing vectors of cycles with their annotations, we can compute a 1-dimensional minimal path homology basis.

According to [1], we have the following: (1) given annotations for edges, the time to compute the annotations of Horton cycles, is $O(n^2g + mn \log n)$; (2) given $O(nm)$ Horton cycles, extracting a minimal homology basis needs $O(nmg^{\omega-1})$ time. Thus in total the time to compute minimal homology basis is $O(rm^{\omega-1} + m^\omega + nmg^{\omega-1})$, where $r = \min\{\mathbf{a}(G)m, m + \sum_{(u,v) \in E} (d_{in}(u) + d_{out}(v))\}$.

5.2 Preliminary experimental results

We implemented our algorithms to compute both the 1-dimensional path homology and the 1-dimensional persistent path homology. The implementaion is in Python 3 using the coefficient field $\mathbb{F} = \mathbb{R}$.

5.2.1 Comparing our algorithm with previous algorithm

We test on some datasets on both our software ⁴ as well as the software in [6] ⁵, including U.S. economic sector data, cycle network, C.elegans, Citeseer and Cora. All experiments are worked on a PC Macbook Pro with Processor 2.9GHz Intel Core i5, Memory 8GB 1867 MHz DDR3. We first introduce the datasets, and then analyse the output.

U.S. economic sector data This dataset is released by the U.S. Bureau of Economic Analysis(<https://www.bea.gov/>) of the “make” and “use” tables of the production of commodities by industries. We obtained “use” table data for 15 industries across the year range 1997-2015; we have 19 tables, each showing the yearly asymmetric flow of commodities across industries. We used same preprocessing used by [6], after which we get 19 complete directed graphs.

Asian migration and remittance This dataset is the Asian net migration and remittance networks in 2015 including 50 countries and regions, obtained from UN Global Migration Database and on bilateral remittances from the World Bank database as reported respectively in [24] and [23]. [16] analyzed the data via directed clique complex. Here we use the same preprocessing as [16] and work on persistent path homology.

Directed cycle graph with 1000 vertices This dataset is a directed cycle graph with 1000 vertices. Each edge follows in the same direction; for every vertex, both the indegree and outdegree are exactly 1.

C.elegans This dataset is a chemical synapse network of C.elegans [25]. It is a directed graph with 279 vertices and 2194 edges. Each vertex represents a neuron, and every edge reflects the synaptic contact between corresponding neurons; the source is the sender, and the sink is the receiver. Every edge has an weight, meaning the number of chemical synapse the receiver received from the sender.

Citation networks–Citeseer and Cora [22] These two datasets are both citation benchmarks. Both are directed networks, indicating the citation between papers. There are 2708 vertices and 5429 edges in Cora, while 3279 vertices and 4608 edges in Citeseer.

Dataset Name	Our algorithm(s)	Algorithm in [6](s)
U.S.economic sector data(19 graphs)	0.7381(average)	0.4795(average)
Migration	2.1277	3.8396
Remittance	1.7780	2.0914
Directed cycle graph	0.0047	0.8197
C.elegans	21.2429	71.1714
Cora	6.0170	27.3146
Citeseer	2.6352	13.5158

Table 1

Analysis Table 1 summarizes the runtimes for our approach as well as the algorithm in [6]. It implies that the baseline approach has a better performance than ours for small but dense graphs. This is because in dense graphs(e.g. complete graphs), the candidate set we compute in our algorithm is comparable with the size of 2-paths; the term $r \approx \sum_{(u,v) \in E} (d_{in}(u) + d_{out}(v))$ in Theorem 1.1.

⁴Code is available in <https://github.com/tianqicoding/1dPPH>

⁵Code can be found in <https://github.com/samirchowdhury/pph-matlab>

However, our algorithm significantly outperforms the baseline approach for graphs whose edges and vertices are comparable. The reason is that in this case, the term r is determined by $\mathbf{a}(G)m$. In this type of graphs, $\mathbf{a}(G)m$ is smaller than the number of 2-paths. Furthermore, our algorithm performs on large dataset well which makes (persistent) path homology more applicable in real datasets.

5.3 Asian Migration and Remittance

The datasets show the migration and remittance between countries and regions in asia. We list all countries and regions in Table 2.

Order	Country	Abbrev.	Order	Country	Abbrev.
1	Afghanistan	AF	26	Lebanon	LB
2	Armenia	AM	27	Malaysia	MY
3	Azerbaijan	AZ	28	Maldives	MV
4	Bahrain	BA	29	Mongolia	MN
5	Bangladesh	BD	30	Myanmar	MM
6	Bhutan	BT	31	Nepal	NP
7	Brunei Darussalam	BN	32	Oman	OM
8	Cambodia	KH	33	Pakistan	PK
9	China(mainland)	CN	34	Philippines	PH
10	Hong Kong	HK	35	Qatar	QA
11	Macau	MO	36	Republic of Korea	KR
12	Cyprus	CY	37	Saudi Arabia	SA
13	Dem. People’s Rep. of Korea	KP	38	Singapore	SG
14	Georgia	GE	39	Sri Lanka	LK
15	India	IN	40	State of Palestine	PS
16	Indonesia	ID	41	Syria	SY
17	Iran	IR	42	Tajikistan	TJ
18	Iraq	IQ	43	Thailand	TH
19	Israel	IL	44	Timor-Leste	TI
20	Japan	JP	45	Turkey	TR
21	Jordan	JO	46	Turkmenistan	TM
22	Kazakhstan	KZ	47	United Arab Emirates	AE
23	Kuwait	KW	48	Uzbekistan	UZ
24	Kyrgyzstan	KG	49	Vietnam	VN
25	Laos	LA	50	Yemen	YE

Table 2

The persistent path homologies of migration and remittance networks are motivated by flow structure. We are concerned with flows containing single sink and single source. Different with [16], we regard cycles not only with boundary triangle structure but also with boundary quadrangle structure as trivial: two flows with one or two edges from the source to the sink are equivalent. Under this motivation, we capture those non-trivial cycles, as well as compute the persistence.

We first do some preprocess on the dataset as in [16]. For remittance data, let r_{ab} be the remittance from a to b . We create an edge (a, b) if $r((a, b)) = r_{ab} - r_{ba} > 0$; there are no bi-gons in the graph. We set the edge weight $w(e)$ to $w(e) = \max_e(r(e)) + 1 - r(e)$, inducing a filtration of path homologies. The edge weights transform largest remittance to smallest. As a consequence, cycles with large weights are born early, and cycles that are born early but killed off by edges with smaller weights will have large persistence. Same preprocessing is employed on migration

dataset.

We process persistent path homology on migration network. There are 44 generating cycles while there are 61 in [16], meaning that there are 17 generating homology class non-trivial in [16] become trivial now when they are born because of the boundary quadrangles: there are two 2-path flows from the source to the sink. Same as [16], all cycles are killed of at the end, indicating small migration flow across countries and regions within cycles. We listing all generating cycles as Figure 9 and Figure 10. Here all red nodes denote sources, greens denote sinks and blues denote other vertices. Figure 9 and Figure 10 reflect that neighbor countries tend to attract immigrants from the same countries, e.g. there are big migrations from India to both Kuwait and United Arab Emirates. On the other hand, people in neighbor countries, e.g. there are amount of people in both China(mainland) and Philippines moving to Hong Kong and Japan. Besides, we capture a directed cycle Kazakhstan→Kyrgyzstan→ Tajikistan →Kazakhstan, indicating a directed flow.

The generating cycles for remittance network are listed in Figure 9 and Figure 10. Most generating cycles are consistent with cycles in migration generating cycles: the generating cycle for the remittance network is a generating cycle in migration network with all arrows reversed. For example, there is a generating cycle in Figure 9: India→United Arab Emirates←Indonesia→Saudi Arabia←India. It corresponds to a generating cycle in Figure 11: India←United Arab Emirates→Indonesia←Saudi Arabia→India. The guess behind that could be after migration, people tend to send money back to home.

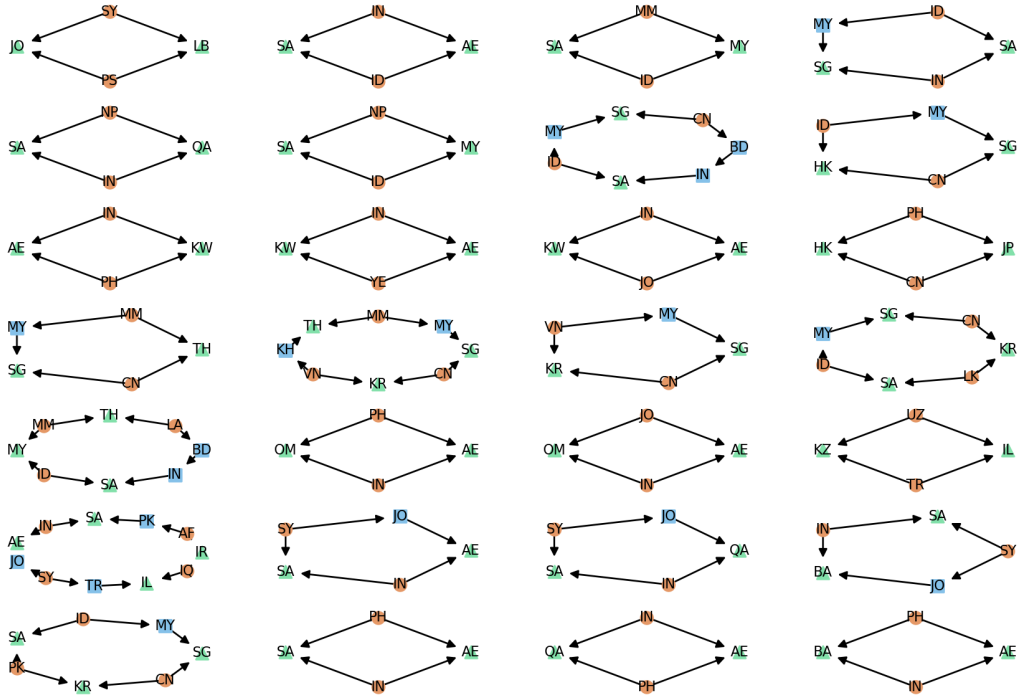


Figure 9: Generating cycles for persistent path homology on migration network

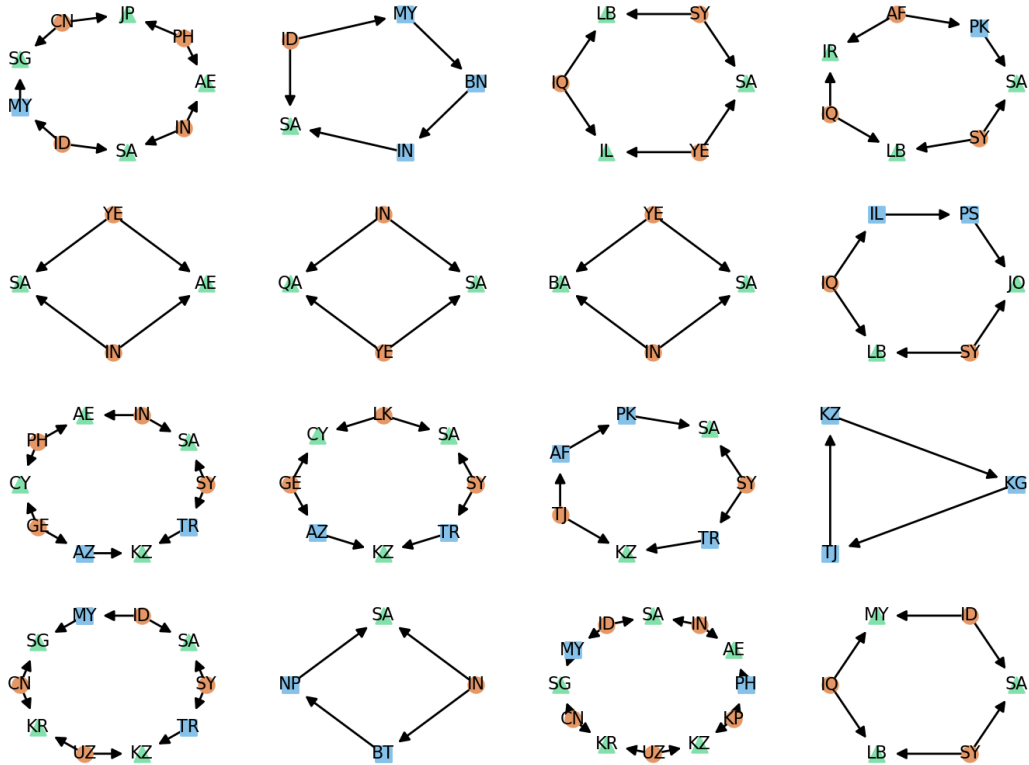


Figure 10: Generating cycles for persistent path homology on migration network(cont.)

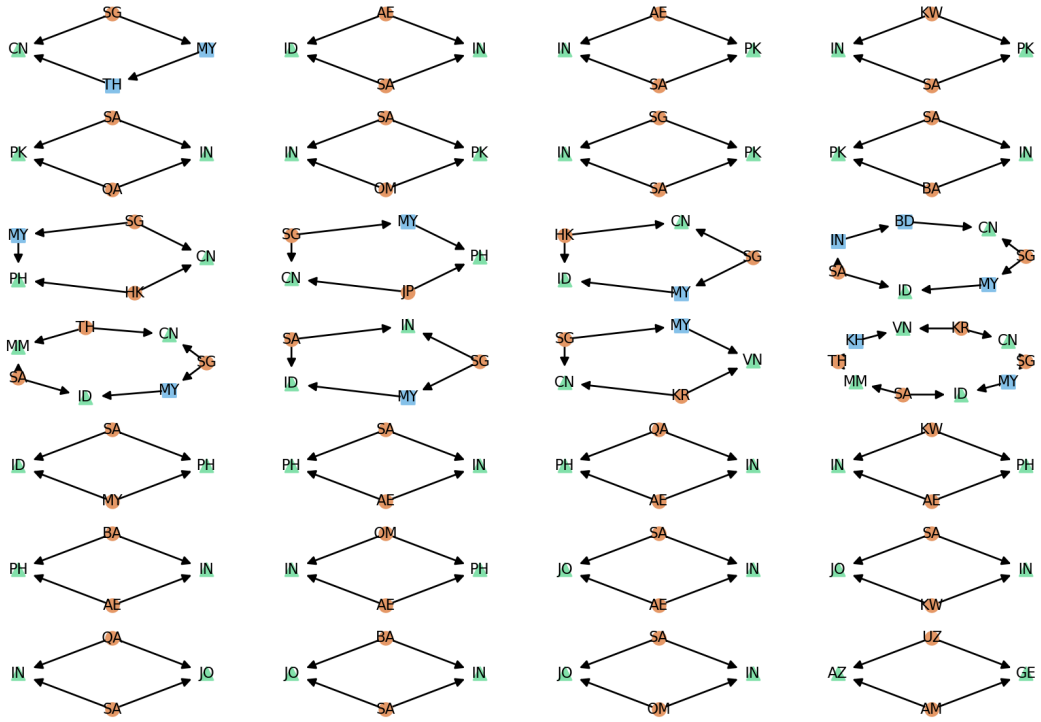


Figure 11: Generating cycles for persistent path homology on remittance network

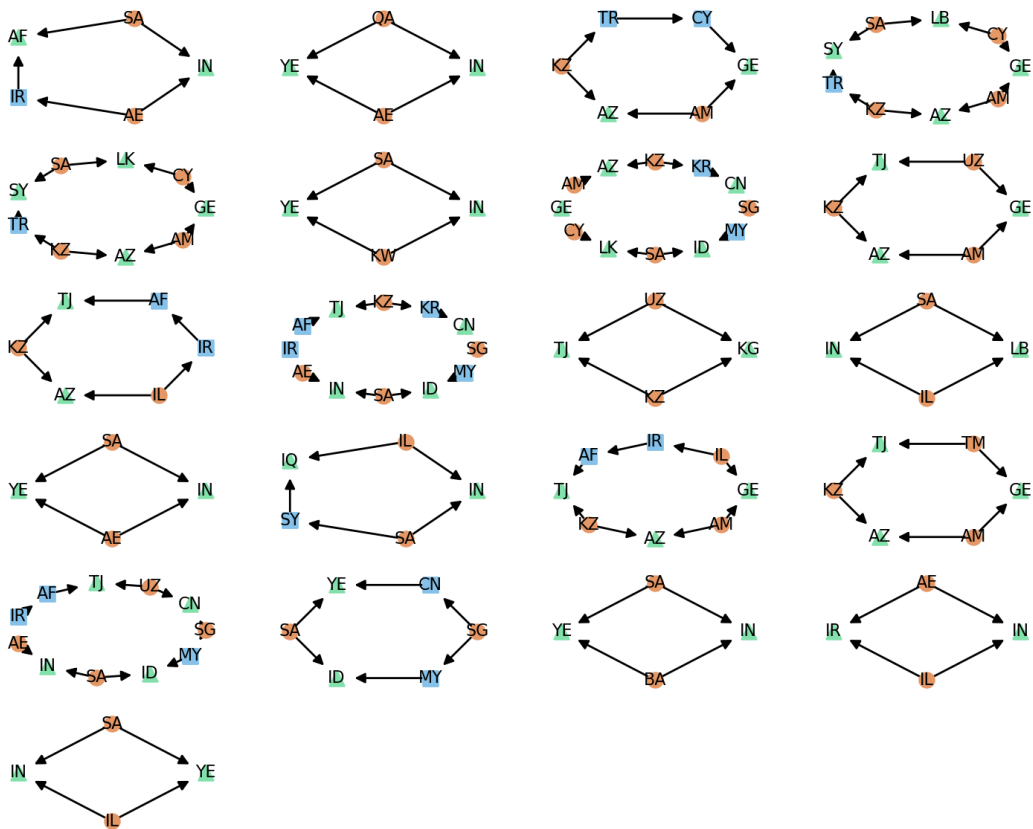


Figure 12: Generating cycles for persistent path homology on remittance network(cont.)

5.4 C.elegans

Path homology. We first compute the 1-dimensional path homology of this network. The rank of 1-dimensional homology is 17, whereas it is reported in [21] that the rank of 1-dimensional directed cliques is 183. This means that boundary quadrangles have a great effect on the synaptic contact structure; there are a number of cycles that can be written as linear combination of boundary triangles and quadrangles, but cannot be represented only by boundary triangles.

We also compare with the 1-dimensional path homology on a set of 1000 directed Erdoš-Reñyi random graphs with 279 vertices and the connection probability 0.028 (thus with 2194 expected connections). The average first betti number of these ER random graphs is 114.91, while the first betti number in C.elegance is 17. It supports the claim from [25] that the C.elegance graph is significantly different from Erdoš-Reñyi random graph with the same number of vertices and similar number of edges.

Minimal homology basis. We also computed the minimum homology basis (with respect to lengths of cycles) for the C.elegans network. Interestingly, all the 17 generating cycles in the computed minimal homology basis are (non-boundary) *quadrangles*. Furthermore, there are no triangles or quadrangles which are directed cycles. However, when we tested on 1000 Erdoš-Reñyi random graphs, we found that each of them has directed triangles or quadrangles in its respective minimal homology basis. Our results provide some information on four neuron subnetworks for the chemical synapse network for C.elegans (the analysis of four neuron subnetworks is of interest and was previously carried out for the gap-junction network of C.elegans [25]).

6 Concluding remarks

A natural question is whether it is possible to have a more efficient algorithm for computing (persistent) path homology of higher dimensions improving the work of [6]. Another question is whether we can compute a minimal path homology basis faster improving our current time bound $O(m^\omega n)$.

Acknowledgement. The authors thank anonymous reviewers for helpful comments on this paper. This work is in part supported by National Science Foundation under grants CCF-1740761, DMS-1547357, and RI-1815697.

References

- [1] Busaryev, O., Cabello, S., Chen, C., Dey, T.K., Wang, Y.: Annotating simplices with a homology basis and its applications. In: Algorithm Theory – SWAT 2012. pp. 189–200. Springer Berlin Heidelberg, Berlin, Heidelberg (2012)
- [2] Chen, W., Wang, Y., Yang, S.: Efficient influence maximization in social networks. In: Proceedings of the 15th ACM SIGKDD international conference on Knowledge discovery and data mining. pp. 199–208. ACM (2009)
- [3] Cheung, H.Y., Kwok, T.C., Lau, L.C.: Fast matrix rank algorithms and applications. Journal of the ACM (JACM) **60**(5), 31 (2013)
- [4] Chiba, N., Nishizeki, T.: Arboricity and subgraph listing algorithms. SIAM Journal on Computing **14**(1), 210–223 (1985)
- [5] Chowdhury, S., Mémoli, F.: A functorial dower theorem and persistent homology of asymmetric networks. Journal of Applied and Computational Topology **2**(1-2), 115–175 (2018)

- [6] Chowdhury, S., Mémoli, F.: Persistent path homology of directed networks. In: Proceedings of the Twenty-Ninth Annual ACM-SIAM Symposium on Discrete Algorithms. pp. 1152–1169. SIAM (2018)
- [7] Cohen-Steiner, D., Edelsbrunner, H., Morozov, D.: Vines and vineyards by updating persistence in linear time. In: Proceedings of the twenty-second annual symposium on Computational geometry. pp. 119–126. ACM (2006)
- [8] Dey, T.K., Li, T., Wang, Y.: Efficient algorithms for computing a minimal homology basis. In: Latin American Symposium on Theoretical Informatics. pp. 376–398 (2018)
- [9] Dlotko, P., Hess, K., Levi, R., Nolte, M., Reimann, M., Scolamiero, M., Turner, K., Muller, E., Markram, H.: Topological analysis of the connectome of digital reconstructions of neural microcircuits. arXiv preprint arXiv:1601.01580 (2016)
- [10] Erickson, J., Whittlesey, K.: Greedy optimal homotopy and homology generators. In: Proceedings of the sixteenth annual ACM-SIAM symposium on Discrete algorithms. pp. 1038–1046. Society for Industrial and Applied Mathematics (2005)
- [11] Grigor’yan, A., Lin, Y., Muranov, Y., Yau, S.T.: Homologies of path complexes and digraphs. arXiv preprint arXiv:1207.2834 (2012)
- [12] Grigor’yan, A., Lin, Y., Muranov, Y., Yau, S.T.: Homotopy theory for digraphs. arXiv preprint arXiv:1407.0234 (2014)
- [13] Grigor’yan, A., Lin, Y., Muranov, Y., Yau, S.T.: Cohomology of digraphs and (undirected) graphs. *Asian J. Math* **19**(5), 887–931 (2015)
- [14] Harary, F.: Graph Theory. Addison Wesley series in mathematics, Addison-Wesley (1971), <https://books.google.com/books?id=q80WtwEACAAJ>
- [15] Horton, J.D.: A polynomial-time algorithm to find the shortest cycle basis of a graph. *SIAM Journal on Computing* **16**(2), 358–366 (1987)
- [16] Ignacio, P.S.P., Darcy, I.K.: Tracing patterns and shapes in remittance and migration networks via persistent homology. *EPJ Data Science* **8**(1), 1 (2019)
- [17] Jeannerod, C.: LSP matrix decomposition revisited (2006), <http://www.ens-lyon.fr/LIP/Pub/Rapports/RR/RR2006/RR2006-28.pdf>.
- [18] Liebchen, C., Rizzi, R.: A greedy approach to compute a minimum cycle basis of a directed graph. *Information Processing Letters* **94**(3), 107–112 (2005)
- [19] Masulli, P., Villa, A.E.: The topology of the directed clique complex as a network invariant. *SpringerPlus* **5**(1), 388 (2016)
- [20] Milo, R., Shen-Orr, S., Itzkovitz, S., Kashtan, N., Chklovskii, D., Alon, U.: Network motifs: simple building blocks of complex networks. *Science* **298**(5594), 824–827 (2002)
- [21] Reimann, M.W., Nolte, M., Scolamiero, M., Turner, K., Perin, R., Chindemi, G., Dłotko, P., Levi, R., Hess, K., Markram, H.: Cliques of neurons bound into cavities provide a missing link between structure and function. *Frontiers in computational neuroscience* **11**, 48 (2017)
- [22] Sen, P., Namata, G., Bilgic, M., Getoor, L., Galligher, B., Eliassi-Rad, T.: Collective classification in network data. *AI magazine* **29**(3), 93–93 (2008)

- [23] The International Development Association, t.w.b.g.: Bilateral remittance estimates for 2015 using migrant stocks, host country incomes, and origin country incomes (millions of us\$) (october 2016 version) (2016), <https://www.worldbank.org/en/topic/migrationremittancesdiasporaissues/brief/migration-remittances-data>
- [24] United Nations, D.o.E., (2015), S.A.: United nations department of economic & social affairs pd trends in international migrant stock : migrants by destination and origin (united nations database, pop/db/mig/stock/rev.2015) (2015), <https://www.un.org/en/development/desa/population/migration/data/estimates2/estimates15.asp>
- [25] Varshney, L.R., Chen, B.L., Paniagua, E., Hall, D.H., Chklovskii, D.B.: Structural properties of the caenorhabditis elegans neuronal network. PLoS computational biology **7**(2), e1001066 (2011)

A Proof of Theorem 3.1

Proof. First, by discussions in Section 2.1, it is easy to see that $\mathbf{Q} \subseteq \mathbf{B}_1 \subseteq \mathbf{Z}_1$. We now show that $\mathbf{B}_1 \subseteq \mathbf{Q}$. To this end, consider any 2-path (2-chain) $p = \sum a_{uvw} \cdot e_{uvw} \in \Omega_2$, where $a_{uvw} \in \mathbb{F}$ is the coefficient of the elementary 2-path e_{uvw} . Its boundary is $\partial p = \sum a_{uvw}(e_{uv} - e_{uw} + e_{vw})$ which we will argue to be in the space \mathbf{Q} . Now set $C = \partial p$.

Specifically, consider an elementary 2-path e_{uvw} in C such that $a_{uvw} \neq 0$. We have that $\partial e_{uvw} = e_{uv} - e_{uw} + e_{vw}$. Note that at this point, we do not yet know whether the allowed 2-path e_{uvw} is also an ∂ -invariant path yet (i.e, it is not clear whether $\partial e_{uvw} \in \Omega_1$). Nevertheless, as e_{uvw} is an allowable 2-path, edges $(u, v), (v, w) \in E$ (that is, both 1-paths e_{uv} and e_{vw} are allowed). As for the 1-path e_{uw} , we have three cases:

(i) $u = w$, we have a bi-gon.

(ii) $u \neq w$ and (u, w) is an edge in G . In this case, $e_{uv} - e_{uw} + e_{vw}$ is allowed. As it is also a cycle, it follows that $e_{uv} - e_{uw} + e_{vw} \in \Omega_1$, and in fact, it forms a boundary triangle.

(iii) $u \neq w$ and $(u, w) \notin E$: In this case, e_{uvw} cannot exist in ∂C because $C \in \Omega_2$, meaning that ∂C must be an allowed 1-path. In other words, e_{uvw} has to be cancelled by the boundary of some other elementary 2-path $e_{uv'w}$ with $a_{uv'w} \neq 0$ in C . Since $(u, w) \notin E$, the 2-path $e_{uv'w}$ is not a bi-gon nor a boundary triangle. That is, there is a 2-chain $e_{uv'w}$ with $a_{uv'w} \neq 0$, whose boundary equals $e_{uv'} - e_{uw} + e_{v'w}$, and $(u, v'), (v'w) \in E$. Hence $\partial(e_{uvw} - e_{uv'w}) = e_{uv} + e_{vw} - e_{uv'} - e_{v'w}$ forms a boundary quadrangle.

We now update $C' = C - a_{uvw}e_{uvw}$ for cases (i) and (ii), or update $C' = C - a_{uvw}(e_{uvw} - e_{uv'w})$ for case (iii). It is easy to see that C' contains fewer terms with non-zero coefficients than C . We repeat the above argument to C' till it becomes the zero. As a result, $C = \partial p$ is decomposed to be a combination of bi-gons, boundary triangles and boundary quadrangles. It follows that for any 2-chain $p \in \Omega_2$, we have its boundary $\partial p \in \mathbf{Q}$, which proves $\mathbf{B}_1 \subset \mathbf{Q}$. Putting everything together, we have that $\mathbf{B}_1 = \mathbf{Q}$.

□